Available online at www.sciencedirect.com
SCIENCE DIRECT
International Journal of Mass Spectrometry 249–250 (2006) 359–363
International Journal of Mass Spectrometry
www.elsevier.com/locate/ijms

Gas-phase proton transfer from dications: Coulombic repulsion between reaction products in $C_{60}H^{2+}$ + B (B = C_3H_3N, HCN and CO)

Jeremy N. Harvey *, Christine Bathelt

School of Chemistry and Centre for Computational Chemistry, University of Bristol, Cantock's Close, BS8 1TS Bristol, UK

Received 27 October 2005; received in revised form 2 December 2005; accepted 2 December 2005
Available online 9 January 2006

This paper is dedicated to the memory of Chava Lifshitz.

Abstract

B3LYP/6-311+G**//B3LYP/6-31G* calculations are carried out on C_{60}^{z+} species (z = 0–3), $C_{60}H^+$, $C_{60}H^{2+}$ and on the potential energy surfaces for proton transfer from $C_{60}H^{2+}$ to CH_2CHCN, HCN and CO. Reasonable agreement is obtained with experiment for the C_{60} species, although the second and third ionization potentials are too low. The calculated potential energy surfaces account for observed reactivity. Analysis of the charge distribution in the TS for proton transfer to HCN helps explain the origin of the Coulombic barrier.

Keywords: Dication; Proton transfer; Computation; Electronic structure

1. Introduction

The ion chemistry of carbon clusters such as C_{60} is a particularly rich area of mass spectrometry, and was the subject of a recent review by Lifshitz [1]. Typical reactions of fullerene ions involve loss of C_2 fragments. Where the initial cluster bears more than one positive charge, such processes can lead to Coulombic explosion through production of C_2^+. These processes are identified through the large kinetic energy release of the fragments.

Another very interesting charge fission reaction of fullerene derivatives has been studied in detail by Petrie et al., namely transfer of a proton from the dication $C_{60}H^{2+}$ [2] and trications $C_{60}XH^{3+}$ (where XH is, e.g., NH_3, OH_2) [3] to bases of varying strength. These ions are in some respects surprisingly unreactive, with $C_{60}H^{2+}$ unable to transfer a proton to neutrals such as CS_2 or C_2H_4, despite the fact that these are expected to have a higher proton affinity than C_{60}^+. This was explained by the presence of a Coulombic barrier to dissociation to form the protonated base and the fullerene monocation, which is only surmounted when the base has a considerably larger proton affinity than required for exothermic reaction. This feature of the potential energy surface, typical in reactions of multiply charged ions [4], is shown schematically in Fig. 1. The reaction proceeds through initial formation of an ion–molecule complex between the dication and the neutral, followed by proton transfer and charge separation. The height of the latter barrier with respect to the products can be rationalized using a model in which one charge is localized on the proton being transferred, and the other is located on the opposite side of the fullerene cage. Assuming that the TS is located close to the encounter complex $C_{60}H^{2+}\cdots B$, then this leads to a charge–charge distance of 8.0 ± 0.7 Å [2]. Given that the charges interact roughly in vacuo, this leads to a predicted reverse barrier of 42 ± 4 kcal/mol. This value can then be used to correct the apparent proton affinity (or gas-phase basicity) of $C_{60}H^{2+}$ to give the 'correct' thermodynamic value.

Proton transfer was observed to occur slowly for $CH_2(CN)_2$, CH_2O and HCN, which have respective gas-phase basicities of 167.4, 164.3 and 163.8 kcal/mol, whereas no reaction was observed with CS_2 (GB = 158 kcal/mol) and other weaker bases. This corresponds to an apparent gas-phase basicity of 166 ± 4 kcal/mol [2]. Using the estimated barrier due to Coulomb repulsion discussed above, this can be translated into a 'real' gas-phase basicity of 124 ± 8 kcal/mol, much lower than the apparent one. However, this value is dependent on the accuracy of the model. It is of interest to see how well this model describes reactivity in this type of system, as it can also yield

* Corresponding author. Tel.: +44 117 9546991; fax: +44 117 9251295.
E-mail address: jeremy.harvey@bris.ac.uk (J.N. Harvey).

1387-3806/$ – see front matter © 2005 Elsevier B.V. All rights reserved.
doi:10.1016/j.ijms.2005.12.002

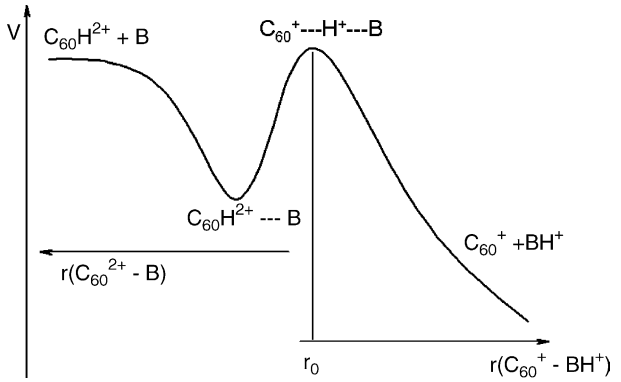

Fig. 1. Potential energy surfaces involved in gas-phase proton transfer from a dication such as $C_{60}H^{2+}$ to a neutral base.

insight into gas-phase deprotonation reactions of other multiply charged ions, especially the highly charged protein ions which are formed in electrospray ionization processes. We note that the experimental work expresses proton affinities as gas-phase basicities, that is, gas-phase free energies at room temperature for the reaction $C_{60}H^{2+} \rightarrow C_{60}^{+} + H^{+}$. With some assumptions about entropic contributions, the proton affinity (enthalpy of the same reaction) can be derived as 134 ± 8 kcal/mol [2]. We will use proton affinities rather than free energies in the results section of this work.

We are interested in using computation to assess the structure, energetics and reactivity of gas-phase dications and other multiply charged ions [5–10]. In particular, we have examined potential energy surfaces for proton transfer from NeH^{+} to the LaO^{+} cation to form the dication $LaOH^{2+}$ [6]. Although this proton transfer is exothermic, it is unlikely to occur due to the large Coulombic repulsion as the two reactants approach each other. In this work, we examine proton transfer from $C_{60}H^{2+}$ to three bases studied in the experimental work of Petrie et al. [2], namely CH_2=CH–CN, HCN and CO. These species have proton affinities of respectively 187.5, 170.4 and 140.0 kcal/mol [11], and were observed to undergo respectively efficient, slow and no proton transfer [2]. We have also studied the series of ions C_{60}^{z+} ($z = 0$–3), and examined the electronic structure of the proton transfer TSs to elucidate whether or not the model proposed in the experimental study is accurate. Previous computational work has addressed C_{60} and some of its ions using semiempirical [12] and DFT [13] methods, but none to our knowledge has addressed $C_{60}H^{2+}$ or its reactions.

2. Computational details

All calculations have been carried out at using the standard B3LYP hybrid density functional as implemented in the Jaguar 4.0 program [14]. The unrestricted ansatz (UB3LYP) was used for all open-shell species. All geometries were optimized using the 6-31G* basis on all atoms, and single-point calculations were then carried out at these optimized geometries using the larger 6-311+G** basis. Due to computational restrictions, it was not possible to carry out frequency calculations on the large C_{60} system, so unless mentioned otherwise, reported energies are based on electronic energies only. However, in some cases, zero point energy corrections are included, and these were obtained either directly, or, for C_{60} and its derivatives, from B3LYP/6-31G* frequency analysis of a model compound, the bowl-shaped fullerene fragment $C_{26}H_{12}$ (diindeno[1,2,3,4-*defg*,1′,2′,3′,4′-*mnop*]chrysene, [15]) shown in Scheme 1. Population analysis was carried out using single-point calculations at the B3LYP/6-311G** level.

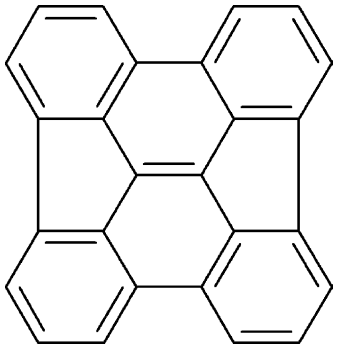

Scheme 1.

3. Results

We have first computed ionization potentials for C_{60}, C_{60}^{+}, C_{60}^{2+} and $C_{60}H^{+}$, as shown in Table 1. In all cases, the larger basis set leads to a better description of the species with lower charge, and hence to a higher ionization energy. B3LYP is in very good agreement with experiment for the first ionization potential of C_{60} when using the larger basis set. The second ionization potential, corresponding to formation of triplet C_{60}^{2+}, is less accurate, as it is too small by ca. 0.7 eV. The tendency of DFT methods to underestimate second ionization potentials for hydrocarbons has been noted before [16], and can be attributed to errors associated with electron self-interaction and the incorrect behaviour of the long-range potential for the electron. The *third* ionization potential, leading to quartet C_{60}^{3+}, is smaller than the experimental value by as much as 2 eV, which even though the experimental error bar is fairly large represents a huge margin of error. $C_{60}H^{+}$ is a closed-shell species, so better agreement with experiment for its ionization potential might be expected, and is indeed observed. It is to be noted, however, that the experimental value shown here is derived from the proton affinity of C_{60}^{+} through the use of a thermodynamic cycle, and is thereby to be taken with caution as the proton affinity itself depends on the accuracy of the model discussed above.

Table 1
Computed and experimental ionization energies (eV) of C_{60} species

	B3LYP/6-31G*	B3LYP/6-311+G**[a]	Experimental
C_{60}	7.41	7.72	7.61 ± 0.02 [17]
C_{60}^{+}	10.37	10.68	11.39 ± 0.05 [18]
C_{60}^{2+}	13.64	13.79	15.6 ± 0.5 [19]
$C_{60}H^{+}$	10.28	10.55	10.70 ± 0.4 [2]

[a] Single-point energy at the B3LYP/6-31G* geometry.

Table 2
Computed and experimental proton affinities (kcal/mol) of C_{60} species, model hydrocarbons and co-reactants

	B3LYP/6-31G*	B3LYP/6-311+G**[a]	Exp
Naphthalene	207.9 (200.5)	202.7 (195.4)	191.9 [11]
Anthracene	225.3 (217.3)	219.8 (211.8)	209.7 [11]
Perylene	229.7 (221.8)	224.1 (216.2)	212.4 [11]
$C_{26}H_{12}$	214.7 (207.8)	209.4 (202.5)	–
C_{60}[b]	212.3 (205.3)	204.2 (197.1)	205.5 ± 1.5 [20]
C_{60}^{+}[b]	146.1 (138.5)	139.0 (131.4)	134 ± 8 [2]
CH_2CHCN	196.9 (190.2)	195.0 (188.2)	187.5 [11]
HCN	175.9 (168.7)	174.5 (167.2)	170.4 [11]
CO	148.0 (140.8)	146.0 (138.8)	142.0 [11]

[a] Single-point energy at the B3LYP/6-31G* geometry.
[b] Zero-point energy correction taken from calculations on $C_{26}H_{12}$ species of Scheme 1.

We next consider the proton affinities of the species involved in this study, as well as the hydrocarbons benzene, anthracene and perylene and the bowl-shaped fullerene fragment $C_{26}H_{12}$ (Table 2). The agreement with experiment is fair for the reference compounds, especially with the larger basis set (the small basis set values may be affected by basis set superposition error). Somewhat unexpectedly, given the accuracy for the reference species, the agreement with experiment is less good for C_{60}, which has a predicted proton affinity of 197.1 kcal/mol, roughly 8 kcal/mol smaller than the experimental value [20]. The latter was determined by FT-ICR bracketing experiments, with proton transfer observed to occur from NH_4^+ (PA = 204 kcal/mol) to gas-phase C_{60}, but not from hexamethylbenzene (PA = 207 kcal/mol). In these experiments, the gas-phase C_{60} is generated by heating solid C_{60} to 400 Centigrade in a solids probe and may therefore contain significant thermal energy, which can in principle lead to proton transfer even from bases with a slightly higher proton affinity. It is therefore possible that the experimental value is a bit too high, although a computational error of this magnitude is of course conceivable also. The proton affinity of C_{60}^+ is within the error bounds of the experimental value, but as for the ionization potential of $C_{60}H^+$, this observation should be taken with caution given the assumptions made in deriving the latter.

We now turn to the calculated potential energy surfaces for proton transfer from $C_{60}H^{2+}$ to the three bases, CH_2CHCN, HCN and CO. The qualitative shape of these surfaces is shown in Fig. 1, with the computed energetics summarized in Table 3.

Both cyanoethene and hydrocyanic acid form relatively strong ion–molecule encounter complexes, with hydrogen bonding between the acidic hydrogen on the fullerene and the basic nitrogen ($r_{H–N}$ of respectively 1.94 and 2.11 Å). Carbon monoxide, with its smaller proton affinity and smaller dipole, forms a much weaker adduct, with a low bond energy for dissociation of the carbon monoxide, and a long C–H contact of 2.37 Å. For HCN, we also investigated the energy of bound adducts in which the nucleophilic nitrogen atom forms a bond to a carbon atom of the fullerene cage. These isomeric adducts all lie significantly higher in energy and have not been further considered.

Table 3
B3LYP/6-311+G**//B3LYP/6-31G* computed potential energy surfaces (kcal/mol) for proton transfer from $C_{60}H^{2+}$ to bases CH_2CHCN, HCN and CO

	CH_2CHCN	HCN	CO
E_{rel} ($C_{60}H^{2+}$ + B)	0.0 (0.0)	0.0 (0.0)	0.0 (0.0)
E_{rel} ($C_{60}H^{2+}\cdots$B)	−14.5 (−16.8)	−9.6 (−11.7)	−0.9 (−2.7)
E_{rel} (TS $C_{60}^{+}\cdots H^{+}\cdots$B)	−10.9 (−9.0)	−0.4 (−0.3)	30.6 (33.8)
E_{rel} (C_{60}^{+} + BH^{+})	−56.0 (−50.9)	−35.5 (−29.9)	−7.0 (−1.9)
Reverse barrier	45.1 (41.9)	35.1 (29.6)	37.6 (35.7)

Values in parentheses refer to B3LYP/6-31G* calculations.

The transition states for proton transfer all have the expected structure, with the protonated co-reactant beginning to move away from C_{60}^+. As the reaction with cyanoethene is the most exothermic, the transition state in this case is quite early, with the C_{60}^+–H^+ bond not yet completely broken nor the N–H bond completely formed ($r_{C–H}$ = 1.40 Å, $r_{H–N}$ = 1.34 Å). With HCN and CO, in contrast, the new N–H and C–H bonds are completely formed (1.05 and 1.10 Å, respectively), whereas the C–H bond is broken (2.12 and 3.00 Å, respectively). The structure of the TS for reaction with HCN is shown in Fig. 2.

The relative energy of the proton transfer TSs varies quite strongly between the three reactions. The barrier decreases as proton transfer becomes more exothermic, lying much higher in energy than reactants for CO, roughly at the same energy for HCN, and well below for cyanoethene. This is in good agreement with the observed experimental behaviour [2]. Proton transfer will not occur to CO under thermal conditions given the high barrier. With the TS lying at the same energy as the entrance channel for HCN, proton transfer will depend upon the angle of approach of reactants, and on the dynamics within the encounter complex, for HCN. As a consequence, reaction will be observed but with a low efficiency. With cyanoethene, however, the low barrier, barely higher than the encounter complex, will ensure that almost every collision leads to product formation.

It can be noted in Table 3 that the height of the proton transfer TSs with respect to products (the reverse barrier height) is fairly similar in all three cases. This provides support for the model used in the experimental paper [2], whereby this barrier is due almost entirely to electrostatic charge–charge interactions between the separating singly charged fragments. The reverse barrier is highest in the case of the reaction with cyanoethene.

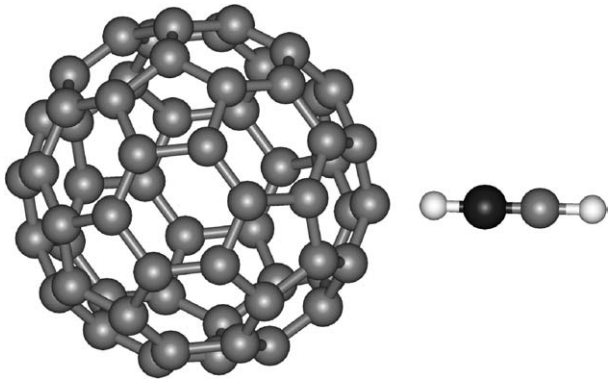

Fig. 2. Optimised geometry of the TS for proton transfer from $C_{60}H^{2+}$ to HCN.

This can be readily understood in terms of the electrostatic model: this TS, as already noted, is very early and hence involves a fairly short distance between the protonated cyanoethene and C_{60}^+ fragments.

We use population analysis to characterize the electronic structure of the TS in the case of HCN. Both Mulliken and NBO partial charges were computed for each atom at the TS at the B3LYP/6-311G** level, and give similar results. Results are given below for the Mulliken analysis first, with the NBO value in paretheses. As expected, the total charge on the C_{60}^+ fragment is close to one, at 1.082 (1.049), indicating that the electronic character at the TS involves near-total charge transfer to the base, as assumed in the previous model. The charge on the nascent $HCNH^+$ product is 0.918 (0.951). The distribution of the charge within each fragment is however considerably different from that assumed in the model of Petrie and Bohme [2]. The centroid of the charge on the $HCNH^+$ product lies close to the carbon atom, at a distance of 0.439 Å (0.388 Å) towards the nitrogen atom, and is thereby very close to the centre of mass of the ion. As such, it is much further away from the fullerene cage than assumed, at a distance of 3.875 Å (3.926 Å) from the nearest carbon atom, as compared to the 1 Å distance assumed in the model. This is because proton transfer has already occurred completely at the TS, so the charge is located on the whole $HCNH^+$ moiety, not just the transferred proton. Also, the $HCNH^+$ has already started to move away from the fullerene cage, as noted above. The charge centroid of the fullerene lies close to the centre of the cage, displaced by only 1.174 Å (1.203 Å) away from its centre of mass in a direction opposite to that of the departing $HCNH^+$. In the model, the charge was assumed to be polarized entirely to the other side of the fullerene. Evidently, such localization, whilst it would decrease the Coulombic repulsion, would also lead to a severe loss of resonance energy. This would be very unfavourable in energetic terms, and instead, the fullerene cation is only moderately polarized.

Despite these quite large differences, the charge–charge distance is in fact fairly close to that predicted by the model, with the charge centroids on the $HCNH^+$ and C_{60}^+ fragments lying 8.643 Å (8.721 Å) apart, which compares favourably to the 8 Å assumed in the model. This explains why the DFT-calculated height of the reverse barrier, 35 kcal/mol, is fairly close to the value predicted with the simple model, of 42 kcal/mol. Using the DFT derived positions and magnitudes of the charges on the two fragments, the simple charge-repulsion model gives a reverse barrier height of 38.2 kcal/mol (38.0 kcal/mol) which is in even better agreement with the DFT energy. This shows that the reverse barrier is indeed due almost only to charge–charge repulsion, with geometric strain, polarization, etc. playing only a minor role. This is almost certainly true also for the barrier involved in electron transfer from neutral species to C_{60}^{2+} and C_{70}^{2+} [21]. These reactions have been found to occur for neutral species with an ionization energy below 9.25 eV. Given the experimental second ionization potential of 11.39 eV [18], this means there is a barrier in the exit channel of ca. 1.2 eV with respect to ionic products. In turn, this suggests a charge–charge separation of ca. 12 Å. If the charge on the fullerene cage is polarized to a similar extent to that calculated here, this suggests a critical distance between the cage and the electron transfer partner of 7–9 Å.

4. Conclusions

This study is aimed at trying to understand the nature of the Coulombic repulsion barrier to proton transfer in gas-phase reactions of dications, in particular $C_{60}H^{2+}$, with neutral species. This is a model for important charge loss processes such as dissociation of C_2^+ from multiply charged fullerene cages, or evaporation of charge from a multiply charged droplet containing a protein and solvent. Calculations at the B3LYP level of theory reproduce the ionization and proton affinity energetics of C_{60} and several model hydrocarbons reasonably well. The worst discrepancy concerns the second and third ionization potentials of C_{60}. The relative energies of the transition states for deprotonation of $C_{60}H^{2+}$ by CH_2CHCN, HCN and CO are in good agreement with the experimentally observed reactivity. The calculations provide additional insight into the origin of the barrier for proton transfer. Population analysis at the TS shows that the departing charged fragment slightly polarizes the C_{60}^+ co-fragment, but not to the extent assumed in the experimental model. The positive charge on the $HCNH^+$ fragment is however situated much further away from the cage than in the model, so that the assumed charge–charge distance in the model is fairly close to that calculated here. In other cases such as multiply charged proteins, electronic polarizability is unlikely to be much larger than that of the C_{60}^+ ion considered here, so the Coulombic barrier to deprotonation will be best described as involving a protein fragment with the charge distributed roughly evenly over the whole species. This will lead to large barriers to deprotonation and fairly high apparent gas-phase basicities.

Acknowledgement

This work was supported by the European Union as a part of the “MCInet” research and training network.

References

[1] C. Lifshitz, Int. J. Mass Spectrom. 200 (2000) 423.
[2] S. Petrie, G. Javahery, H. Wincel, D.K. Bohme, J. Am. Chem. Soc. 115 (1993) 6290.
[3] S. Petrie, D.K. Bohme, J. Am. Soc. Mass Spectrom. 9 (1998) 114.
[4] D. Schröder, H. Schwarz, J. Phys. Chem. A 103 (1999) 7385.
[5] D. Schröder, J.N. Harvey, H. Schwarz, J. Phys. Chem. A 102 (1998) 3639.
[6] D. Schröder, H. Schwarz, J.N. Harvey, J. Phys. Chem. A 104 (2000) 11257.
[7] D. Schröder, M. Engeser, H. Schwarz, J.N. Harvey, Chem. Phys. Chem. 3 (2002) 583.
[8] M. Kaczorowska, J.N. Harvey, Phys. Chem. Chem. Phys. 4 (2002) 5227.
[9] D. Ascenzi, P. Franceschi, P. Tosi, D. Bassi, M. Kaczorowska, J.N. Harvey, J. Chem. Phys. 118 (2003) 2159.
[10] J.N. Harvey, M. Kaczorowska, Int. J. Mass Spectrom. 228 (2003) 517.
[11] P.J. Linstrom, W.G. Mallard (Eds.), NIST Chemistry WebBook, NIST Standard Reference Database Number 69, June 2005.
[12] See e.g. O.V. Boltalina, I.N. Ioffe, L.N. Sidorov, G. Seifert, K. Vietze, J. Am. Chem. Soc. 122 (2000) 9745.
[13] S. Díaz-Tendero, M. Alcamí, F. Martín, J. Chem. Phys. 119 (2003) 5545.

[14] Jaguar 4.1, Schrodinger, Inc., Portland, OR, USA, 2000.
[15] H.E. Bronstein, N. Choi, L.T. Scott, J. Am. Chem. Soc. 124 (2002) 8870.
[16] D. Schröder, J. Loos, H. Schwarz, R. Thissen, D.V. Preda, L.T. Scott, D. Caraiman, M.V. Frach, D.K. Bohme, Helv. Chim. Acta 84 (2001) 1625.
[17] J.A. Zimmermann, J.R. Eyler, S.B.H. Bach, S.W. McElvany, J. Chem. Phys. 94 (1991) 3556.
[18] H. Steger, J. de Vries, B. Kamke, T. Drewello, Chem. Phys. Lett. 194 (1992) 452.
[19] G. Javahery, H. Wincel, S. Petrie, D.K. Bohme, Chem. Phys. Lett. 204 (1993) 467.
[20] S.W. McElvany, J.H. Callahan, J. Phys. Chem. 95 (1991) 6186.
[21] S. Petrie, G. Javahery, J. Wang, D.K. Bohme, J. Phys. Chem. 96 (1992) 6121.